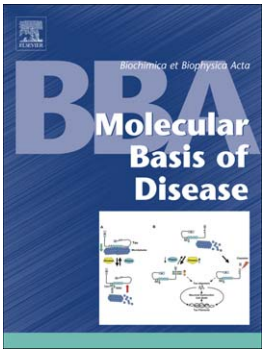

TLR4 Knockout Attenuated High Fat Diet-Induced Cardiac Dysfunction via NF-κB/JNK-Dependent Activation of Autophagy

Nan Hu, Yingmei Zhang

PII: S0925-4439(17)30015-7
DOI: doi:10.1016/j.bbadis.2017.01.010
Reference: BBADIS 64661

To appear in: *BBA - Molecular Basis of Disease*

Received date: 12 October 2016
Revised date: 9 January 2017
Accepted date: 12 January 2017

Please cite this article as: Nan Hu, Yingmei Zhang, TLR4 Knockout Attenuated High Fat Diet-Induced Cardiac Dysfunction via NF-κB/JNK-Dependent Activation of Autophagy, *BBA - Molecular Basis of Disease* (2017), doi:10.1016/j.bbadis.2017.01.010

TLR4 Knockout Attenuated High Fat Diet-Induced Cardiac Dysfunction via NF-κB/JNK-Dependent Activation of Autophagy

Nan Hu[1,2] and Yingmei Zhang[1,2]

[1]Department of Cardiology, Zhongshan Hospital, Fudan University, Shanghai 200032, China;

[2]Center for Cardiovascular Research and Alternative Medicine, University of Wyoming College of Health Sciences, Laramie, WY 82071, USA

Running title: TLR4 and obesity-induced cardiac dysfunction

Correspondence should be addressed to:

Yingmei Zhang, M.D., Ph.D.

Professor, Department of Cardiology, Shanghai Institute of Cardiovascular Diseases, Zhongshan Hospital, Fudan University, Shanghai 200032, China

Tel: 86-13468974520; E-mail: zhangym197951@126.com

ABSTRACT

Obesity is commonly associated with a low grade systematic inflammation, which may contribute to the onset and development of myocardial remodeling and contractile dysfunction. Toll-like receptor 4 (TLR4) plays an important role in innate immunity and inflammation although its role in high fat diet-induced obesity cardiac dysfunction remains elusive. This study was designed to examine the effect of TLR4 ablation on high fat diet intake-induced cardiac anomalies, if any, and underlying mechanism(s) involved. Wild-type (WT) and TLR4 knockout mice were fed normal or high fat (60% calorie from fat) diet for 12 weeks prior to assessment of mechanical and intracellular Ca^{2+} properties. The inflammatory signaling proteins (TLR4, NF-κB, and JNK) and autophagic markers (Atg5, Atg12, LC3B and p62) were evaluated. Our results revealed that high fat diet intake promoted obesity, marked decrease in fractional shortening, and cardiomyocyte contractile capacity with dampened intracellular Ca^{2+} release and clearance, elevated ROS generation and oxidative stress as measured by aconitase activity, the effects of which were significantly attenuated by TLR4 knockout. In addition, high fat intake downregulated levels of Atg5, Atg12 and LC3B, while increasing p62 accumulation. TLR4 knockout itself did not affect Atg5, Atg12, LC3B and p62 levels while it reconciled high fat diet intake-induced changes in autophagy. In addition, TLR4 knockout alleviated high fat diet-induced phosphorylation of IKKβ, JNK and mTOR. *In vitro* study revealed that palmitic acid suppressed cardiomyocyte contractile function, the effect of which was inhibited the TLR4 inhibitor CLI-095, the JNK inhibitor AS601245 or the NF-κB inhibitor Celastrol. Taken together, these data showed that TLR4 knockout ameliorated high fat diet-induced cardiac contractile and intracellular Ca^{2+} anomalies through inhibition of inflammation and ROS, possibly through a NF-κB/JNK-dependent activation of autophagy.

Key words: high fat diet, heart, contractile function, TLR4, autophagy.

1. INTRODUCTION

Obesity is a prevalent global medical problem afflicting more than one third of adults in the United States and the rest of world [1-3]. Obesity, if uncorrected, is known to be associated with increased risk for a myriad of health problems, including insulin resistance, type 2 diabetes, sleep dyspnea, coronary heart disease, stroke, hypertension, and cancer [2]. As one of the most severe hallmarks for obesity, low grade chronic inflammation elicits detrimental consequences on the onset and development of metabolic syndrome associated with myocardial abnormalities [4, 5]. Along the same line, sustained myocardial inflammation may impose severe challenge to myocardium, leading to compromised cardiac function and heart failure.

Toll-like receptors (TLRs) are a family of receptors with a critical role in the activation of innate immune response to lipopolysaccharide. Toll-like receptor 4 (TLR4), in particular, is a unique receptor for the innate immune system found in multiple cell types including immune cells, vasculature and cardiomyocytes [6, 7]. Ample of experimental evidence has depicted a role for TLR4 in the induction of proinflammatory and antiviral cytokines. The proinflammatory reaction following TLR4 activation is believed to be mediated through a myeloid differentiation primary response gene 88 (MyD88)- or toll/interleukin-1 receptor domain-containing adapter protein (TRIF)-dependent mechanism to turn on key transcription factors of pro-inflammatory cytokines [8]. Meanwhile, TLR4 may directly activate essential inflammatory pathways, such as the Jun N-terminal kinase (JNK) and NF-κB, to maintain the low-grade chronic inflammatory state [9-11]. In consequence, these pro-inflammatory cues often lead to dysregulation of intrinsic cellular homeostasis. As one of the critical homeostatic regulators, autophagy plays a pivotal role in the maintenance of subcellular organelle homeostasis and degradation. Autophagy regulates cellular components in immune responses [12]. Moreover, autophagy may participate in cellular

inflammatory responses through clearance of aged or injured mitochondria, a primary site for reactive oxygen species (ROS) production [10]. Mitochondrial ROS is well known to govern inflammasome activation and processing of cytoplasmic targets [13]. However, whether a link exists between TLR4 signaling and obesity-associated dysregulation of myocardial autophagy is unknown. In this study, we hypothesize that TLR4 signaling is involved in the development of myocardial dysfunction in high fat diet-induced obesity. To this end, our objectives were: 1) to determine whether mice lacking functional TLR4 will be protected against peripheral and cardiac derangements during high fat diet-induced obesity and, 2) to identify the underlying intracellular signaling pathways.

2. MATERIALS AND METHODS

2.1. Experimental animals, model of insulin resistance and intraperitoneal glucose tolerance tests (IPGTT): Experimental procedures used here were approved by the Zhongshan Hospital Fudan University (Shanghai, China) and University of Wyoming Institutional Animal Use and Care Committees. Toll-like receptor 4 knockout ($TLR4^{-/-}$) and C57BL/6J (WT) mice were randomly allocated to be fed either a control diet (10% kcal from fat) or a high-fat diet (60% kcal from fat) diet (Research Diets Inc., New Brunswick, NJ) *ad libitum* for 12 weeks. Following a 12-hour fast, 2.0 g/kg glucose was administered intraperitoneally and blood was drawn immediately before and 30, 60, 90, and 120 min after glucose injection. Blood glucose levels were assessed using an Accu-Chek glucose analyzer (Roche Diagnostics, Indianapolis, IN) [14].

2.2 Metabolic measurements: Mice were housed individually in metabolic cages, acclimated for 24 hrs to minimize the novelty effect, and then monitored for 24 hrs in 12-hour light/dark cycle

by indirect open-circuit calorimetry (Oxymax System; Columbus Instruments, Columbus, OH). Metabolic examination was performed over the course of 3 days while respective diet was maintained. Calibration of the calorimeter was performed at the beginning of each measurement day. Oxygen consumption and carbon dioxide production were measured by volume every 10 minutes. Respiratory exchange ratio (RER) was calculated as the ratio of VCO_2/VO_2. Energy expenditure was calculated as $(3.815 + 1.232 \times RER) \times VO_2$ and was normalized to body weight [15].

2.3 Echocardiographic assessment: Cardiac geometry and contractile function were evaluated in anesthetized (ketamine 80 mg/kg and xylazine 12 mg/kg, i.p.) mice using a 2-dimensional (2-D) guided M-mode echocardiography (Phillips Sonos 5500) equipped with a 15–6 MHz linear transducer (Phillips Medical Systems, Andover, MD). Adequate depth of anesthesia was monitored using toe reflex. The heart was imaged in the 2-D mode in the parasternal long-axis view with a depth setting of 2 cm. The M-mode cursor was positioned perpendicular to interventricular septum and posterior wall of left ventricle (LV) at the level of papillary muscles from the 2-D mode. The sweep speed was 100 mm/sec for the M-mode. Diastolic wall thickness, left ventricular (LV) end diastolic dimension (EDD) and LV end systolic dimension (ESD) were measured. All measurements were done from leading edge to leading edge in accordance with the Guidelines of the American Society of Echocardiography. LV fractional shortening was calculated as [(EDD-ESD)/EDD] × 100 [16].

2.4 Cardiomyocyte isolation and cell mechanics: Hearts were removed rapidly from mice sedated with ketamine (80 mg/kg, ip) and xylazine (12 mg/kg, ip) and perfused with oxygenated

(5% CO_2 /95% O_2) Ca^{2+}-free Tyrode's solution containing (in mM): NaCl 135, KCl 4.0, MgCl2 1.0, HEPES 10, NaH2PO4 0.33, glucose 10, butanedione monoxime 10. Hearts were digested with Tyrode's solution containing Liberase Blendzyme TH (Hoffmann-La Roche Inc, Indianapolis, IN) for 15 min. After removal and mincing of the left ventricle, Ca^{2+} was added back to a final concentration of 1.25 mM. Extracellular Ca^{2+} was added incrementally back to 1.2 mM. Normally, a yield of 70–80% viable rod-shaped cardiomyocytes with clear sarcomere striations was achieved. Only rod-shaped myocytes with clear edges were selected for our mechanical and intracellular Ca^{2+} studies. Cardiomyocytes were used within 6 hrs of isolation. Cardiomyocytes with no spontaneous contractions and clear edges were used for shortening and Ca^{2+} cycling experiments. The IonOptix soft-edge system (IonOptix, Milton, MA) was employed to assess the mechanical properties of isolated myocytes. Myocytes were mounted on the stage of an Olympus IX-70 microscope in contractile buffer containing (in mM) 131 NaCl, 4 KCl, 1$CaCl_2$, 1 $MgCl_2$, 10 glucose, and 10 HEPES. Myocytes were stimulated at 0.5 Hz using a pair of platinum wires placed on opposite sides of the chamber and connected to an electrical stimulator (FHC Inc, Brunswick, NE). An IonOptix software was used to capture changes in cell length during shortening and relengthening. Cell shortening and relengthening were assessed using the following indices: peak shortening (PS), maximal velocities of cell shortening and relengthening (±dL/dt), time-to-PS (TPS), and time-to-90% relengthening (TR_{90}) [17].

2.5 Intracellular Ca^{2+} transient: Cardiomyocytes were loaded with fura-2/AM (0.5μM) for 20 min and fluorescence measurements were recorded with dual-excitation fluorescence photo multiplier system (Ionoptix). Cardiomyocytes were placed on an Olympus IX-70 inverted microscope and imaged through a Fluor 40× oil objective. Cells were exposed to light emitted by

a 75-W lamp and passed through either 360 nm or a 380 nm filter, while being stimulated to contract at 0.5Hz. Fluorescence emissions were detected between 480 nm and 520 nm by a photo multiplier tube after first illuminating the cells at a 360 nm 0.5 sec, then at 380 nm for the duration of the recording protocol (333Hz sampling rate). The 360 nm excitation scan can be repeated at the end of the protocol and qualitative changes in intracellular Ca^{2+} concentration were inferred from the ratio of fura-2 fluorescence intensity at two wavelengths (360/380). Fluorescence decay time was assessed as an indication of intracellular Ca^{2+} clearing rate. Single exponential curve fit was applied to calculate the intracellular decay Ca^{2+} constant [18].

2.6 Intracellular reactive oxygen species (ROS): Production of ROS was evaluated by changes in the fluorescence intensity resulted from oxidation of the intracellular fluoroprobe 5-(and -6)-chloromethyl-2',7'-dichlorodihydrofluorescein diacetate (CM-H_2DCF-DA, Molecular Probes, Eugene, OR). In brief, cardiomyocytes were incubated with 25 μM CM-H_2DCF-DA for 30 min at 37^{o}C. The cells were then rinsed and the fluorescence intensity was measured using a fluorescent micro-plate reader at the excitation and emission wavelengths of 480nm and 530 nm respectively (Molecular Devices, Sunnyvale, CA). Untreated cells without fluorescence were used to determine the background fluorescence. The final results were expressed as the ratio of the fluorescent intensity to respective protein content [17].

2.7 Aconitase activity: The aconitase-340 assay^{TM} measures NADPH formation, a product of the oxidation of isocitrate to α-ketoglutarate. Mitochondria prepared from whole heart homogenate were resuspended in 0.2 mM sodium citrate. After determination of protein content, aconitase activity assay (Aconitase activity assay kit, Aconitase-340 assay^{TM}, Oxisresearch, Portland, OR)

was performed according to manufacturer instructions with minor modifications. Briefly, mitochondrial sample (50 µl) was mixed in a 96-well plate with 50 µl trisodium citrate (substrate) in Tris-HCl pH 7.4,50 µl isocitrate dehydrogenase (enzyme) in Tris-HCl, and 50 µl NADP in Tris-HCl. After incubating for 15 min at 37°c with 50 rpm shaking, the absorbance was dynamically recorded at 340 nm every min for 5 min with a spectramax 190 microplate spectrophotometer. During the assay, citrate is isomerized by aconitase into isocitrate and eventually α-ketoglutarate. Tris-HCl buffer (pH 7.4) served as a blank. All results were normalized to respective protein content [19].

2.8 Western blot analysis: Expression of the proinflammatory signaling molecules IKKβ and JNK, as well as the autophagy markers AMPK, mTOR, Atg5, Atg12, LC3B, Atg5 and p62 were assessed. In brief, left ventricular tissue was sonicated in a lysis buffer containing (in mM): TRIS 10, NaCl 150, EDTA 5, 1%Triton X-100 and protease inhibitor cocktail followed by centrifugation at 12,000g for 10 min. Equal amount (30 µg) protein was separated using 7-15% SDS-polyacrylamide gels in minigel apparatus (Mini-PROTEAN II, Bio-Rad, Hercules, CA), and were transferred to nitrocellulose membranes (0.2 µm pore size, Bio-Rad). Membranes were blocked for 1 hr in 5% nonfat milk before being rinsed in TBS-T. The membranes were incubated overnight at 4^{o}C with primary antibodies (1:1,000) against protein of interest (Santa Cruz Biotechnology, Santa Cruz, CA or Cell Signaling technology, Beverly, MA). After incubation with primary antibodies, blots were incubated with horseradish peroxidase-linked secondary antibodies (1:5,000) for 60 min at room temperature. Immunoreactive bands were detected using Super Signal West Dura Extended Duration Substrate (Pierce, Milwaukee, WI). The intensity of bands was measured with a scanning densitometer (Model GS-800, Bio-Rad)

coupled with a Bio-Rad personal computer analysis software. GAPDH was used as the loading control [18, 20].

2.9 Statistical analysis: Data were Mean ± SEM. Difference was assessed using one-way analysis of variance (ANOVA) followed by a Tukey's *post hoc* test. A p value < 0.05 was considered statistically significant.

3. **RESULTS**

3.1 Effect of high fat diet on energy expenditure and glucose tolerance in WT and TLR4-/- mice

To correlate high fat diet-induced adiposity with metabolic activity, metabolic rates were measured in the open-circuit indirect calorimetry cages. As shown in Fig. 1, high fat diet feeding decreased oxygen consumption (VO_2), carbon dioxide production (VCO_2) and respiratory exchange ratio (RER) compared to normal diet-fed mice. There was no discernable difference between WT and $TLR4^{-/-}$ mice regardless of the feeding regimen. These results indicated that TLR4 knockout had little effect on high fat diet-induced adiposity. Interestingly, neither high fat diet intake nor $TLR4^{-/-}$, or both, significantly affected total physical activity or heat production (Supplemental Fig. 1).

As shown in Fig. 2A, TLR4 knockout did not affect food intake. Both WT and knockout mice fed the high fat diet gained significantly more weight than those fed normal diet. At the end of the 3-month high fat diet feeding, baseline glucose levels were unchanged for all groups tested. IPGTT curve revealed that fasting blood glucose levels in the normal fat diet–fed mice started to decline after peaking at 15 min, and nearly returned to baseline 120 min after the intraperitoneal

glucose challenge. However, the post-challenge glucose levels remained at much higher levels between 15 and 120 min in the high fat–fed WT and TLR4$^{-/-}$ mice, indicating existence of systematic glucose intolerance (Fig. 2B).

3.2 Effects of high fat diet and TLR4 deficiency on whole heart contractile function

Echocardiographic analysis (Fig. 2C-F) revealed that high fat diet intake significantly increased LV end systolic diameter (LVESD) and LV wall thickness, as well as suppressed fractional shortening without affecting LV end diastolic diameter (LVEDD), the effects of which with the exception of enlarged LV wall thickness were prevented in TLR4$^{-/-}$ mice. Interestingly, TLR4 knockout itself did not affect any of the echocardiographic indices tested.

3.3 Effects of high fat diet and TLR4 deficiency on mechanical and intracellular Ca^{2+} properties of cardiomyocytes

Mechanical properties revealed unchanged resting cell length regardless of the diet or TLR4 knockout ($p > 0.05$). High fat diet intake reduced peak shortening and maximal velocity of shortening/ relengthening (± dL/dt), associated with prolonged TR_{90} ($p < 0.05$ *vs.* normal diet groups) but not TPS, the effects of which were ablated by TLR4 knockout. TLR4 knockout itself did not exert any notable effect on cell mechanics (Fig. 3). To understand the mechanism(s) behind TLR4 knockout-offered cardiac protection, Fura-2 fluorescence was monitored to evaluate intracellular Ca^{2+} handling. Cardiomyocytes displayed significantly reduced intracellular Ca^{2+} release in response to electrical stimuli (ΔFFI) with prolonged intracellular Ca^{2+} decay along with unchanged baseline FFI following high fat diet challenge, the effect of

which was reconciled by TLR4 knockout. $TLR4^{-/-}$ did not alter intracellular Ca^{2+} homeostasis (Fig. 4).

3.4 Effects of high fat diet and TLR4 deficiency on inflammatory factors

To detect the effect of inflammation on TLR4-induced cardioprotection against high fat diet, levels of the inflammatory factors such as IKKβ and JNK were evaluated. As shown in Fig. 5A-B, high fat diet significantly upregulated phosphorylation of the NF-κB inhibitory protein IKKβ and JNK. Although TLR4 knockout did not affect levels (or phosphorylation) of these proinflammatory factors, it mitigated high fat diet-induced changes in these proinflammatory factors.

3.5 Effect of high fat diet and TLR4 deficiency on AMPK-mTOR signaling

To further explore the possible cell signaling mechanisms behind TLR4 knockout-induced protection against obesity, the AMPK-mTOR pathway was examined. Our data shown in Fig. 5C suggested that high fat diet intake reduced AMPK phosphorylation as evidenced by decreased phosphorylated AMPK-to-AMPK ratio, the effect of which was mitigated by TLR4 knockout. mTOR is a downstream target of AMPK. Our data in Fig. 5D revealed that high fat diet elevated mTOR phosphorylation. Although TLR4 knockout itself did not display any response in mTOR phosphorylation, it attenuated high fat diet-induced changes in mTOR phosphorylation. Neither $TLR4^{-/-}$ nor high fat diet, or both, affected pan protein levels of AMPK and mTOR.

3.6 Effects of TLR4 knockout on high fat diet-induced autophagic response

To explore if autophagy contributes to TLR4 knockout-offered cardioprotection against high fat diet challenge, levels of autophagic markers including Atg5, Atg12, LC3B and p62 were

evaluated. Results shown in Fig. 6 depicted that high fat diet intake significantly decreased levels of Atg5, Atg12 and the LC3B II/I ratio while increasing p62 accumulation, the effects of which were attenuated by TLR4 knockout. TLR4 knockout itself did not alter levels of these autophagic markers.

3.7 Effect of TLR4 knockout on high fat diet-induced ROS production and oxidative stress

To examine the potential mechanism behind TLR4-elicited protection against high fat diet-induced cardiac mechanical anomalies, ROS and oxidative stress were evaluated using DCF fluorescence and aconitase activity, respectively, in myocardial tissues from WT and $TLR4^{-/-}$ mice. Results shown in Fig. 7A-B indicated that ROS production was significantly enhanced whereas aconitase activity was overtly reduced following high fat diet challenge ($p < 0.05$ *vs.* normal diet groups). Consistent with its mechanical responses, TLR4 knockout attenuated high fat diet-induced increase in ROS production and dampened aconitase activity.

3.8 Effect of TLR4 inhibition, JNK inhibition and NF-κB inhibition on palmitic acid-induced cardiomyocyte contractile defects

To elucidate a cause-effect relationship of TLR4 receptor and proinflammatory signaling cascades in high fat diet-induced cardiac anomalies, cardiomyocytes isolated from WT mice were exposed to palmitic acid in the presence or absence of the TLR4 inhibitor CLI-095, the JNK inhibitor AS601245 or the NF-κB inhibitor Celastrol. Our data suggested that palmitic acid incubation significantly depressed peak shortening, maximal velocity of shortening/relengthening, and prolong duration of relengthening without affecting resting cell length and duration of shortening. Although CLI-095, AS601245 and Celastrol alone failed to exhibit any effect on

contractile properties in the absence of palmitic acid, these pharmacological inhibitors protected against palmitic acid-induced cardiomyocyte mechanical anomalies (Fig. 8).

4. DISCUSSION

The salient findings from our study suggested that the 3-month 60% high fat diet feeding led to overt obesity, insulin resistance and glucose intolerance, oxidative stress, and metabolic changes (reduced RER) with cardiac remodeling (enlarged LVESD and LV wall thickness) and cardiac contractile dysfunction. Interestingly, systemic TLR4 knockout alleviated high fat diet-induced metabolic abnormalities including cardiac contractile and intracellular Ca^{2+} defect, ROS accumulation, mitochondrial injury, inflammation and autophagy following high fat diet intake. These findings indicated that LTR4 ablation exerts a protective effect against high fat diet-induced cardiac remodeling, contractile and mitochondrial defects possibly through restoration of autophagy and inflammation factors.

In our study, TLR4 knockout did not affect metabolic activities following high fat diet feeding. Our results did not reveal any significant difference in total activity or heat production among all mouse groups. RER denotes the ratio between CO_2 production and O_2 consumption, suggesting the energetic substrate being oxidized [21]. In our hands, the RER value of around 0.8 in the regular lab chow-fed mice suggests the energy source from both fatty acid oxidation and carbohydrate oxidation [22, 23]. With high fat diet intake (60% of energy from fatty acid which offers more lipid relative to 10% from normal lab chow), RER was significantly dropped to around 0.6 compared with regular lab chow group, suggesting a more predominant role for fatty acid as the energy source. Interestingly, TLR4 knockout did not affect high fat diet-induced

changes in RER, indicating that TLR4 knockout may afford protection to the heart independent of high fat diet-induced global regulation of adiposity.

Echocardiographic and cardiomyocyte mechanical observations from our present study revealed enlarged left ventricular end systolic diameter, decreased fractional shortening, peak shortening, and maximal velocity of shortening/relengthening, as well as prolonged relaxation following high fat diet intake. Interestingly, our study revealed that TLR4 knockout attenuated or mitigated high fat diet-induced myocardial dysfunction. Further observation displayed reduced intracellular Ca^{2+} release in response to electrical stimuli (ΔFFI) and prolonged intracellular Ca^{2+} decay in cardiomyocytes from high fat diet-challenged WT mice, the effect of which was reconciled by TLR4 knockout. These findings depicted a role of intracellular Ca^{2+} handling in high fat diet- and TLR4 knockout-induced changes in myocardial contractile function.

The TLR4 knockout murine model offers an advantageous model for pathological study of obesity especially in the realm of chronic inflammation. Interestingly, such adiposity-independent protective effects seen in TLR4 ablation were also noted with inhibition of JNK and NF-κB [24, 25], as evidenced by our in vitro study using palmitic acid challenge. Meanwhile, our data further indicated activated NF-κB following high fat diet challenge as manifested by elevated IKKβ phosphorylation, the effect of which was nullified by TLR4 knockout. These findings favor a role of cytokine and inflammation in TLR4-elicited cytoprotection, consistent with the notion for a role of TLR4 in the regulation of host immune homeostasis and fat diet intake [26-28]. TLR4 knockout is capable of attenuating inflammation through inactivating NF-κB by way of JNK suppression [29, 30]. NF-κB inhibitor was also found to significantly attenuate TNFα-induced cytotoxicity along with preserved TLR4/Myd88 signaling [31, 32]. These data support a role of NF-κB signaling in TLR4 knockout-induced protection against high fat diet-induced cell stress

and inflammation in the heart. Along the same line, in vitro study revealed that inhibition of NF-κB exerted protective effect against palmitic acid reminiscent of TLR4 inhibitor CLI-095.

Our examination indicated that chronic TLR4 knockout alleviated ROS production and mitochondrial injury as depicted by aconitase level. Although ROS may be necessary for normal cellular function and survival, oxidative stress develops when the balance between ROS production and clearance is interrupted [33]. High fat diet-induces superoxide production to promote oxidative stress. Findings from our study revealed that fat diet prompted accumulation of ROS and mitochondrial injury in conjunction with impaired cardiac contraction and intracellular Ca^{2+} handling. Our result revealed that TLR4 may exert its beneficial role in high fat diet through alleviating ROS production and mitochondrial injury.

Autophagy is a conserved cellular mechanism through which mammalian cells degrade and recycle damaged macromolecules and organelles [34, 35]. A role of autophagy has been reported in an array of cardiovascular diseases including obesity, aging, alcoholism and ischemic injury [36-42]. First, our data suggest that TLR4 deficiency may reverse high fat diet-induced AMPK dephosphorylation and mTOR phosphorylation (resulted from downregulated mTOR expression). Inhibition of AMPK is known to stimulate mTOR signaling. Enhanced mTOR phosphorylation directly promotes autophagy. Second, autophagy usually are characterized with autophagosome membrane specific protein light chain 3 (LC3) or Atg8 [43]. Sequestosome-1 (SQSTM, also known as p62) is an adaptor for autophagosome formation. The higher expression of p62 usually means hindering of fusion of autophagosome and lysosome [44, 45]. Data from our study suggest that high fat diet intake suppressed myocardial autophagy as evidence by decreased Atg5, Atg12, LC3II level and the LC3II/LC3I ratio as well as increased p62 in WT mice. TLR4 knockout attenuated or reversed high fat diet-induced responses in autophagy

signaling molecules, suggesting a better role of autophagy in TLR4-induced cardioprotection against high fat diet intake. These findings support a pivotal role of AMPK-dependent mTOR phosphorylation in high fat diet-induced/TLR4-/--accentuated suppression of autophagy. Intriguingly, recent studies revealed that autophagosme marker was significantly elevated while fusion of autophagosome and lysosome was compromised with acute exposure of paraquat and ischemia/reperfusion challenge [46, 47]. These indicate that autophagy may play disparate role in the maintenance of cellular homeostasis under different stress conditions.

5. CLINICAL IMPLICATION AND LIMITATION

Ample clinical and experimental evidence has consolidated cardiac contractile anomalies in obese subject [48, 49]. Obesity has become an epidemic and modifiable risk factor associated with increased cardiovascular anomalies [50]. Interestingly, the initial studies implicating TLR4 as a trigger for metabolic inflammation depicted that long-chain saturated fatty acids found in the diet were capable of turning on TLR4 signal, en route to insulin resistance and inflammatory gene transcription [51]. Large prospective population-based studies have highlighted clinical impact of dietary intake on circulating inflammatory markers such as IL-6, IL-8, TNF-α, ROS generation and NF-κB binding [52]. For example, elevated circulating serum endotoxin levels are predictive for cardiometabolic disorders later in life in obese individuals [53]. In addition, a remarkable interaction was found between plasma LPS binding protein (LBP) and obesity among middle-aged and older Chinese individuals [54]. Previous reports have demonstrated that chronic high fat diet intake, with time, may promote cardiac hypertrophy, fibrosis and pronounced cardiac injury. Therefore, understanding the mechanisms underlying obesity-associated pathophysiology is pertinent for development of therapeutic interventions to curb this epidemic.

In a series of animal model studies, Cani and colleagues showed that chronic, modest elevations (~1.5 fold) in endotoxin may exist in a high-fat/high energy diet challenge or in transgenic obese mice [46, 55]. In these studies, the diet-induced elevations in endotoxin were related to increased fat deposition, systemic and tissue specific inflammation (e.g., liver, skeletal muscle, and adipose tissue) and insulin resistance [56]. Endotoxin can initiate systemic and local inflammation and also result in ROS production upon binding with TLR4 and subsequent activation of NF-κB [57]. Local inflammation and secretion of pro-inflammatory adipokines from visceral adipose tissues then promote the development of cardiometabolic diseases. Although it is beyond the scope of the current study, evidence from both human and experimental studies favors the contribution of metabolic endotoxemia in low-grade inflammation and development of cardiometabolic diseases.

In conclusion, data from our study revealed that chronic TLR4 knockout rescues against high fat diet-induced cardiac contractile and intracellular Ca^{2+} anomalies as well as cell death through a TLR4-dependent mechanism involving interplay between autophagy and stress signals. TLR4 knockout alleviates oxidative stress, mitochondrial injury and inflammation in high fat diet intake. These results may implicate the possible therapeutic potential of TLR4 in the management of cardiac dysfunction in high fat diet-induced obesity. In particular, TLR4-related cascades such as receptors and downstream molecules deserve more attention in the hunt for therapeutic targets against TLR4 signaling.

6. ACKNOWLEDGMENTS

This work was supported in part by the Natural Science Foundation of China 81370195 and 81522004

7. **DISCLOSURES:** None

8. FIGURE LEGENDS

Fig 1: Effect of 12-week high fat (HF) diet intake on (A) day-time oxygen consumption (VO_2); (B) day-time carbon dioxide production (VCO_2); (C) day-time real-time RER; (D) Pooled day-time RER over a 6-hr period; (E) night-time oxygen consumption (VO_2); (F) night-time carbon dioxide production (VCO_2); (G) night-time real-time RER; and (H) Pooled night-time RER over a 6-hr period; in WT and $TLR4^{-/-}$ mice. Mean ± SEM, n = 6- 8 mice per group, * $p < 0.05$ *vs.* WT group.

Fig. 2: Effect of 12-week high fat (HF) diet intake on (A) body weight; (B) serum glucose; (C) left ventricular end diastolic diameter (LVEDD); (D) left ventricular end systolic diameter (LVESD); (E) fractional shortening; and (D) diastolic wall thickness; in WT and $TLR4^{-/-}$ mice. Mean ± SEM, n = 6- 8 mice per group, * $p < 0.05$ *vs.* WT group.

Fig. 3: Effect of 12-week high fat (HF) diet intake on cardiomyocyte contractile properties in WT and $TLR4^{-/-}$ mice. A: Resting cell length; B: Peak shortening (% of resting cell length); C: Maximal velocity of shortening (+ dL/dt); D: Maximal velocity of relengthening (- dL/dt); E: Time-to-peak shortening (TPS); and F: Time-to-90% relengthening (TR_{90}). Mean ± SEM, n = 90 - 100 cells from 3 mice per group, *$p < 0.05$ *vs.* WT group, $^{\#}$ $p < 0.05$ *vs.* WT-HF group.

Fig. 4: Effect of 12-week high fat diet intake on intracellular Ca^{2+} handling in cardiomyocytes from WT and $TLR4^{-/-}$ mice. (A) Baseline fura-2 fluorescence intensity (FFI); (B) peak FFI; (C) change in FFI in response to electrical stimuli (ΔFFI); and (D) single exponential intracellular

Ca^{2+} decay rate. Mean ± SEM, n = 80 - 90 cells from 3 mice per group, *p < 0.05 *vs.* WT group, $^{\#}$p < 0.05 *vs.* WT-HF group.

Fig. 5: Effect of 12-week high fat diet intake on phosphorylation of IKKβ, JNK, AMPK and mTOR in myocardium from WT and $TLR4^{-/-}$ mice. A: phosphorylation of IKKβ normalized to pan protein expression; B: phosphorylation of JNK normalized to pan protein expression; C: phosphorylation of AMPK normalized to pan protein expression; and D: phosphorylation of mTOR normalized to pan protein expression. Mean ± SEM, n = 5-8 hearts per group; *p < 0.05 *vs.* WT group, $^{\#}$p < 0.05 *vs.* WT-HF group.

Fig. 6: Effect of 12-week high fat diet intake on autophagic markers in myocardium from WT and $TLR4^{-/-}$ mice. A: Insets: Representative gel blots of autophagy proteins and GAPDH (used as loading control) using specific antibodies; B: Atg5 level; C: Atg12 level; D: LC3-II level; E: LC3-II to LC3-I ratio; and F: p62 level; Mean ± SEM, n = 5-8 hearts per group; *p < 0.05 *vs.* WT group, $^{\#}$p < 0.05 *vs.* WT-HF group.

Fig. 7: Effect of 12-week high fat diet intake on ROS production and aconitase activity in myocardium from WT and $TLR4^{-/-}$ mice. A: ROS production measured using DCF fluorescence; and B: aconitase activity. Mean ± SEM, n = 5-6 mice per group, *p < 0.05 *vs.* WT group, $^{\#}$ p < 0.05 *vs.* WT-HF group.

Fig. 8: Contractile properties in cardiomyocytes from WT mice treated palmitic acid (PA, 75 μM) in the presence or absence of the TLR4 inhibitor CLI-095 (400 nM), the JNK inhibitor

AS601245 (1 μM) or the NF-κB inhibitor celastrol (1 μM). (A) resting cell length; (B) peak shortening (normalized to resting cell length); (C) maximal velocity of shortening (+dL/dt); (D) maximal velocity of relengthening (−dL/dt); (E) time-to-peak shortening (TPS); and (F) time-to-90% relengthening (TR_{90}). Mean ± SEM, n = 55-60 cells from 3 mice per group, * $p < 0.05$ *vs.* control group, # $p < 0.05$ *vs.* PA group.

REFERENCES

[1] P. Poirier, T.D. Giles, G.A. Bray, Y. Hong, J.S. Stern, F.X. Pi-Sunyer, R.H. Eckel, A. American Heart, P.A. Obesity Committee of the Council on Nutrition, Metabolism, Obesity and cardiovascular disease: pathophysiology, evaluation, and effect of weight loss: an update of the 1997 American Heart Association Scientific Statement on Obesity and Heart Disease from the Obesity Committee of the Council on Nutrition, Physical Activity, and Metabolism, Circulation, 113 (2006) 898-918.

[2] Y. Zhang, J. Ren, Epigenetics and obesity cardiomyopathy: From pathophysiology to prevention and management, Pharmacology & therapeutics, 161 (2016) 52-66.

[3] M.T. Zanella, O. Kohlmann, Jr., A.B. Ribeiro, Treatment of obesity hypertension and diabetes syndrome, Hypertension, 38 (2001) 705-708.

[4] H. Xu, G.T. Barnes, Q. Yang, G. Tan, D. Yang, C.J. Chou, J. Sole, A. Nichols, J.S. Ross, L.A. Tartaglia, H. Chen, Chronic inflammation in fat plays a crucial role in the development of obesity-related insulin resistance, The Journal of clinical investigation, 112 (2003) 1821-1830.

[5] R.S. Vasan, Cardiac function and obesity, Heart, 89 (2003) 1127-1129.

[6] R. Spirig, J. Tsui, S. Shaw, The Emerging Role of TLR and Innate Immunity in Cardiovascular Disease, Cardiology research and practice, 2012 (2012) 181394.

[7] D.M. Tsukumo, M.A. Carvalho-Filho, J.B. Carvalheira, P.O. Prada, S.M. Hirabara, A.A. Schenka, E.P. Araujo, J. Vassallo, R. Curi, L.A. Velloso, M.J. Saad, Loss-of-function mutation in Toll-like receptor 4 prevents diet-induced obesity and insulin resistance, Diabetes, 56 (2007) 1986-1998.

[8] S. Rosa Ramirez, M. Ravi Krishna Dasu, Toll-like receptors and diabetes complications: recent advances, Current diabetes reviews, 8 (2012) 480-488.

[9] B.C. Lee, J. Lee, Cellular and molecular players in adipose tissue inflammation in the development of obesity-induced insulin resistance, Biochimica et biophysica acta, 1842 (2014) 446-462.

[10] D. Cai, M. Yuan, D.F. Frantz, P.A. Melendez, L. Hansen, J. Lee, S.E. Shoelson, Local and systemic insulin resistance resulting from hepatic activation of IKK-beta and NF-kappaB, Nature medicine, 11 (2005) 183-190.

[11] F. Dong, Q. Li, N. Sreejayan, J.M. Nunn, J. Ren, Metallothionein prevents high-fat diet induced cardiac contractile dysfunction: role of peroxisome proliferator activated receptor gamma coactivator 1alpha and mitochondrial biogenesis, Diabetes, 56 (2007) 2201-2212.

[12] X. Xu, Y. Hua, S. Nair, R. Bucala, J. Ren, Macrophage migration inhibitory factor deletion exacerbates pressure overload-induced cardiac hypertrophy through mitigating autophagy, Hypertension, 63 (2014) 490-499.

[13] L. Cao, X. Qin, M.R. Peterson, S.E. Haller, K.A. Wilson, N. Hu, X. Lin, S. Nair, J. Ren, G. He, CARD9 knockout ameliorates myocardial dysfunction associated with high fat diet-induced obesity, Journal of molecular and cellular cardiology, 92 (2016) 185-195.

[14] N. Hu, J. Ren, Y. Zhang, Mitochondrial aldehyde dehydrogenase obliterates insulin resistance-induced cardiac dysfunction through deacetylation of PGC-1alpha, Oncotarget, (2016).

[15] E. Panzhinskiy, Y. Hua, P.A. Lapchak, E. Topchiy, T.E. Lehmann, J. Ren, S. Nair, Novel curcumin derivative CNB-001 mitigates obesity-associated insulin resistance, The Journal of pharmacology and experimental therapeutics, 349 (2014) 248-257.

[16] Y. Zhang, S.A. Babcock, N. Hu, J.R. Maris, H. Wang, J. Ren, Mitochondrial aldehyde dehydrogenase (ALDH2) protects against streptozotocin-induced diabetic cardiomyopathy: role of GSK3beta and mitochondrial function, BMC medicine, 10 (2012) 40.

[17] N. Hu, L. Yang, M. Dong, J. Ren, Y. Zhang, Deficiency in adiponectin exaggerates cigarette smoking exposure-induced cardiac contractile dysfunction: Role of autophagy, Pharmacological research, 100 (2015) 175-189.

[18] J. Ren, J.R. Privratsky, X.P. Yang, F. Dong, E.C. Carlson, Metallothionein alleviates glutathione depletion-induced oxidative caydiomyopathy in murine hearts, Crit Care Med, 36 (2008) 2106-2116.

[19] N. Hu, M. Dong, J. Ren, Hydrogen sulfide alleviates cardiac contractile dysfunction in an Akt2-knockout murine model of insulin resistance: role of mitochondrial injury and apoptosis, American journal of physiology. Regulatory, integrative and comparative physiology, 306 (2014) R761-771.

[20] P. Zhao, S. Turdi, F. Dong, X.Y. Xiao, G.H. Su, X.L. Zhu, G.I. Scott, J. Ren, Cardiac-Specific Overexpression of Insulin-Like Growth Factor I (Igf-1) Rescues Lipopolysaccharide-Induced Cardiac Dysfunction and Activation of Stress Signaling in Murine Cardiomyocytes, Shock, 32 (2009) 100-107.

[21] E. Ferrannini, The theoretical bases of indirect calorimetry: a review, Metabolism: clinical and experimental, 37 (1988) 287-301.

[22] J.E. Oosterman, E. Foppen, R. van der Spek, E. Fliers, A. Kalsbeek, S.E. la Fleur, Timing of fat and liquid sugar intake alters substrate oxidation and food efficiency in male Wistar rats, Chronobiology international, 32 (2015) 289-298.

[23] S. Chung, T. Wong, H. Nagasaki, O. Civelli, Acute homeostatic responses to increased fat consumption in MCH1R knockout mice, Journal of molecular neuroscience : MN, 42 (2010) 459-463.

[24] J.G. Cronin, M.L. Turner, L. Goetze, C.E. Bryant, I.M. Sheldon, Toll-like receptor 4 and MYD88-dependent signaling mechanisms of the innate immune system are essential for the response to lipopolysaccharide by epithelial and stromal cells of the bovine endometrium, Biology of reproduction, 86 (2012) 51.

[25] D. Hildebrand, A. Sahr, S.J. Wolfle, K. Heeg, K.F. Kubatzky, Regulation of Toll-like receptor 4-mediated immune responses through Pasteurella multocida toxin-induced G protein signalling, Cell communication and signaling : CCS, 10 (2012) 22.

[26] W. Wang, M. Deng, X. Liu, W. Ai, Q. Tang, J. Hu, TLR4 activation induces nontolerant inflammatory response in endothelial cells, Inflammation, 34 (2011) 509-518.

[27] C. Wang, X. Ha, W. Li, P. Xu, Y. Gu, T. Wang, Y. Wang, J. Xie, J. Zhang, Correlation of TLR4 and KLF7 in Inflammation Induced by Obesity, Inflammation, (2016).

[28] X. Yang, M. Haghiac, P. Glazebrook, J. Minium, P.M. Catalano, S. Hauguel-de Mouzon, Saturated fatty acids enhance TLR4 immune pathways in human trophoblasts, Human reproduction, 30 (2015) 2152-2159.

[29] O. Takeuchi, S. Akira, Toll-like receptors; their physiological role and signal transduction system, International immunopharmacology, 1 (2001) 625-635.

[30] G. Zhu, Q. Huang, Y. Huang, W. Zheng, J. Hua, S. Yang, J. Zhuang, J. Wang, J. Ye, Lipopolysaccharide increases the release of VEGF-C that enhances cell motility and promotes lymphangiogenesis and lymphatic metastasis through the TLR4- NF-kappaB/JNK pathways in colorectal cancer, Oncotarget, (2016).

[31] Z. Zhou, P. Gengaro, W. Wang, X.Q. Wang, C. Li, S. Faubel, C. Rivard, R.W. Schrier, Role of NF-kappaB and PI 3-kinase/Akt in TNF-alpha-induced cytotoxicity in microvascular endothelial cells, Am J Physiol Renal Physiol, 295 (2008) F932-941.

[32] W.V. Ingman, D.J. Glynn, M.R. Hutchinson, Inflammatory mediators in mastitis and lactation insufficiency, Journal of mammary gland biology and neoplasia, 19 (2014) 161-167.

[33] S.K. Maulik, S. Kumar, Oxidative stress and cardiac hypertrophy: a review, Toxicol Mech Methods, 22 (2012) 359-366.

[34] X. Xu, J. Ren, Unmasking the janus faces of autophagy in obesity-associated insulin resistance and cardiac dysfunction, Clin Exp Pharmacol Physiol, 39 (2012) 200-208.

[35] I. Tanida, Autophagy basics, Microbiol Immunol, 55 (2011) 1-11.

[36] A.B. Gustafsson, R.A. Gottlieb, Autophagy in Ischemic Heart Disease, Circ Res, 104 (2009) 150-158.

[37] J. McCormick, R.A. Knight, S.P. Barry, T.M. Scarabelli, K. Abounit, D.S. Latchman, A. Stephanou, Autophagy in the stress-induced myocardium, Front Biosci (Elite Ed), 4 (2012) 2131-2141.

[38] L. Yan, D.E. Vatner, S.J. Kim, H. Ge, M. Masurekar, W.H. Massover, G. Yang, Y. Matsui, J. Sadoshima, S.F. Vatner, Autophagy in chronically ischemic myocardium, Proc Natl Acad Sci U S A, 102 (2005) 13807-13812.

[39] D. Zhang, R. Contu, M.V. Latronico, J. Zhang, R. Rizzi, D. Catalucci, S. Miyamoto, K. Huang, M. Ceci, Y. Gu, N.D. Dalton, K.L. Peterson, K.L. Guan, J.H. Brown, J. Chen, N. Sonenberg, G. Condorelli, MTORC1 regulates cardiac function and myocyte survival through 4E-BP1 inhibition in mice, The Journal of clinical investigation, 120 (2010) 2805-2816.

[40] B.A. Rothermel, J.A. Hill, Autophagy in load-induced heart disease, Circ Res, 103 (2008) 1363-1369.

[41] C.H. Hsieh, P.Y. Pai, H.W. Hsueh, S.S. Yuan, Y.C. Hsieh, Complete induction of autophagy is essential for cardioprotection in sepsis, Ann Surg, 253 (2011) 1190-1200.

[42] D. Dutta, R. Calvani, R. Bernabei, C. Leeuwenburgh, E. Marzetti, Contribution of impaired mitochondrial autophagy to cardiac aging: mechanisms and therapeutic opportunities, Circ Res, 110 (2012) 1125-1138.

[43] Z. Yang, D.J. Klionsky, An overview of the molecular mechanism of autophagy, Curr Top Microbiol Immunol, 335 (2009) 1-32.

[44] M.L. Seibenhener, T. Geetha, M.W. Wooten, Sequestosome 1/p62--more than just a scaffold, FEBS Lett, 581 (2007) 175-179.

[45] J. Moscat, M.T. Diaz-Meco, M.W. Wooten, Signal integration and diversification through the p62 scaffold protein, Trends Biochem Sci, 32 (2007) 95-100.

[46] P.D. Cani, R. Bibiloni, C. Knauf, A. Waget, A.M. Neyrinck, N.M. Delzenne, R. Burcelin, Changes in gut microbiota control metabolic endotoxemia-induced inflammation in high-fat diet-induced obesity and diabetes in mice, Diabetes, 57 (2008) 1470-1481.

[47] S. Wang, X. Zhu, L. Xiong, Y. Zhang, J. Ren, Toll-like receptor 4 knockout alleviates paraquat-induced cardiomyocyte contractile dysfunction through an autophagy-dependent mechanism, Toxicology letters, 257 (2016) 11-22.

[48] A.F. Ceylan-Isik, M.R. Kandadi, X. Xu, Y. Hua, A.J. Chicco, J. Ren, S. Nair, Apelin administration ameliorates high fat diet-induced cardiac hypertrophy and contractile dysfunction, Journal of molecular and cellular cardiology, 63 (2013) 4-13.

[49] R. Guo, Y. Zhang, S. Turdi, J. Ren, Adiponectin knockout accentuates high fat diet-induced obesity and cardiac dysfunction: role of autophagy, Biochimica et biophysica acta, 1832 (2013) 1136-1148.

[50] J.P. Despres, Body fat distribution and risk of cardiovascular disease: an update, Circulation, 126 (2012) 1301-1313.

[51] L.A. Velloso, F. Folli, M.J. Saad, TLR4 at the Crossroads of Nutrients, Gut Microbiota, and Metabolic Inflammation, Endocrine reviews, 36 (2015) 245-271.

[52] K.T. Teng, C.Y. Chang, L.F. Chang, K. Nesaretnam, Modulation of obesity-induced inflammation by dietary fats: mechanisms and clinical evidence, Nutrition journal, 13 (2014) 12.

[53] K.A. Kallio, K.A. Hatonen, M. Lehto, V. Salomaa, S. Mannisto, P.J. Pussinen, Endotoxemia, nutrition, and cardiometabolic disorders, Acta diabetologica, 52 (2015) 395-404.

[54] X. Liu, L. Lu, P. Yao, Y. Ma, F. Wang, Q. Jin, X. Ye, H. Li, F.B. Hu, L. Sun, X. Lin, Lipopolysaccharide binding protein, obesity status and incidence of metabolic syndrome: a prospective study among middle-aged and older Chinese, Diabetologia, 57 (2014) 1834-1841.

[55] P.D. Cani, J. Amar, M.A. Iglesias, M. Poggi, C. Knauf, D. Bastelica, A.M. Neyrinck, F. Fava, K.M. Tuohy, C. Chabo, A. Waget, E. Delmee, B. Cousin, T. Sulpice, B. Chamontin, J. Ferrieres, J.F. Tanti, G.R. Gibson, L. Casteilla, N.M. Delzenne, M.C. Alessi, R. Burcelin, Metabolic endotoxemia initiates obesity and insulin resistance, Diabetes, 56 (2007) 1761-1772.

[56] U.J. Jung, M.S. Choi, Obesity and its metabolic complications: the role of adipokines and the relationship between obesity, inflammation, insulin resistance, dyslipidemia and nonalcoholic fatty liver disease, International journal of molecular sciences, 15 (2014) 6184-6223.

[57] R. Meli, G. Mattace Raso, A. Calignano, Role of innate immune response in non-alcoholic Fatty liver disease: metabolic complications and therapeutic tools, Frontiers in immunology, 5 (2014) 177.

COMPETING INTERESTS: None

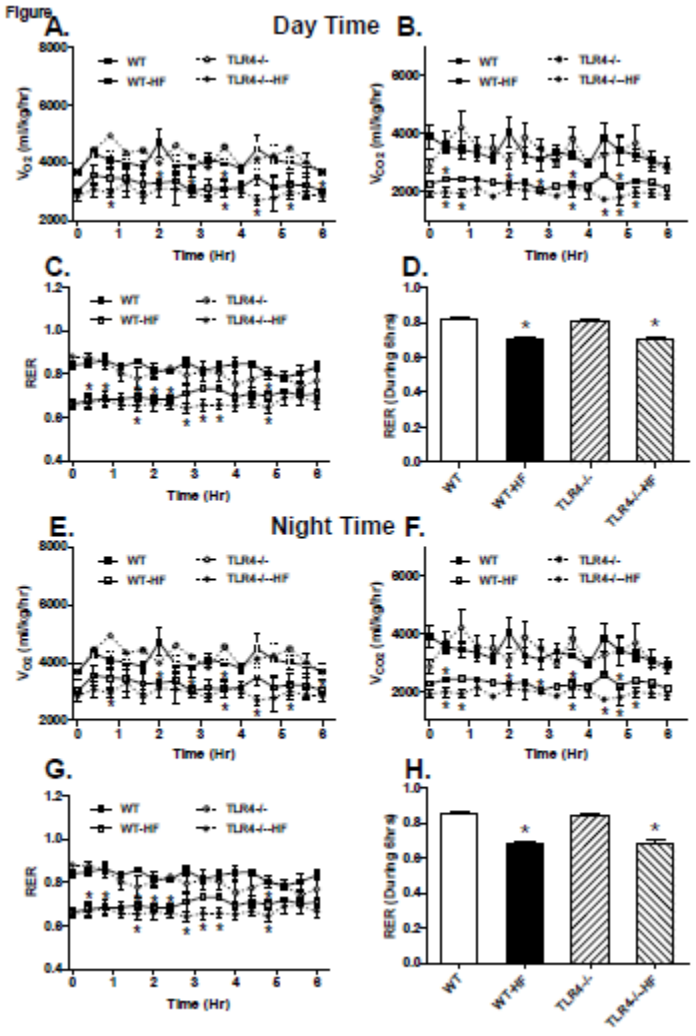
Figure
A.
Day Time
B.
C.
D.
E.
Night Time
F.
G.
H.
WT
WT-HF
TLR4-/-
TLR4-/--HF
Time (Hr)
RER
RER (During 6hrs)

Fig. 1

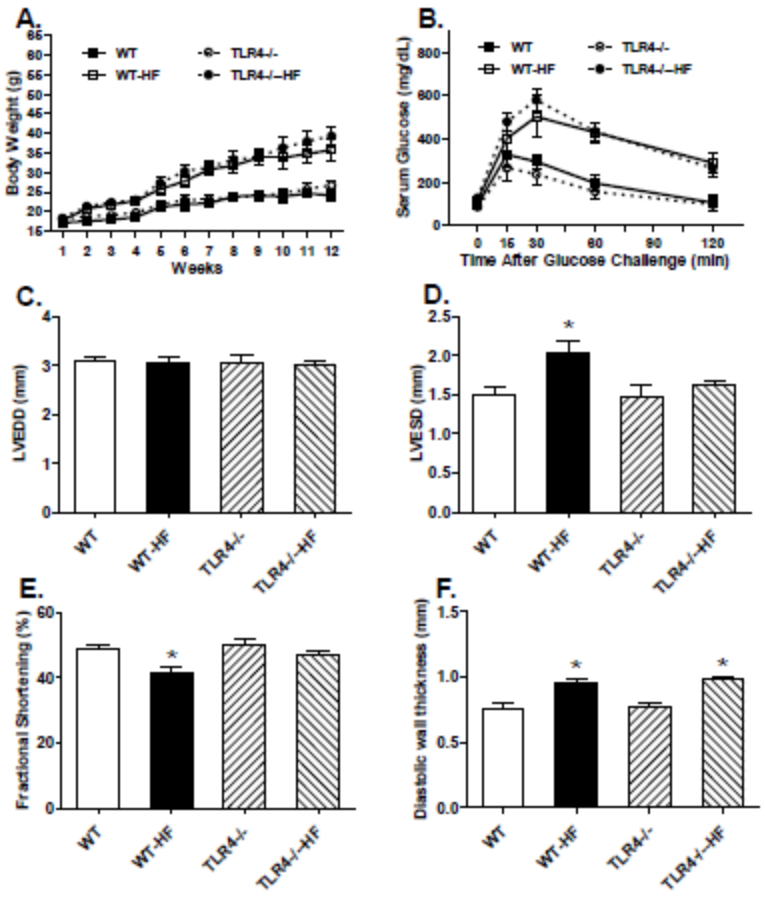
A.
Body Weight (g)
Weeks
WT
WT-HF
TLR4-/-
TLR4-/-HF
B.
Serum Glucose (mg/dL)
Time After Glucose Challenge (min)
C.
LVEDD (mm)
D.
LVESD (mm)
E.
Fractional Shortening (%)
F.
Diastolic wall thickness (mm)

Fig. 2

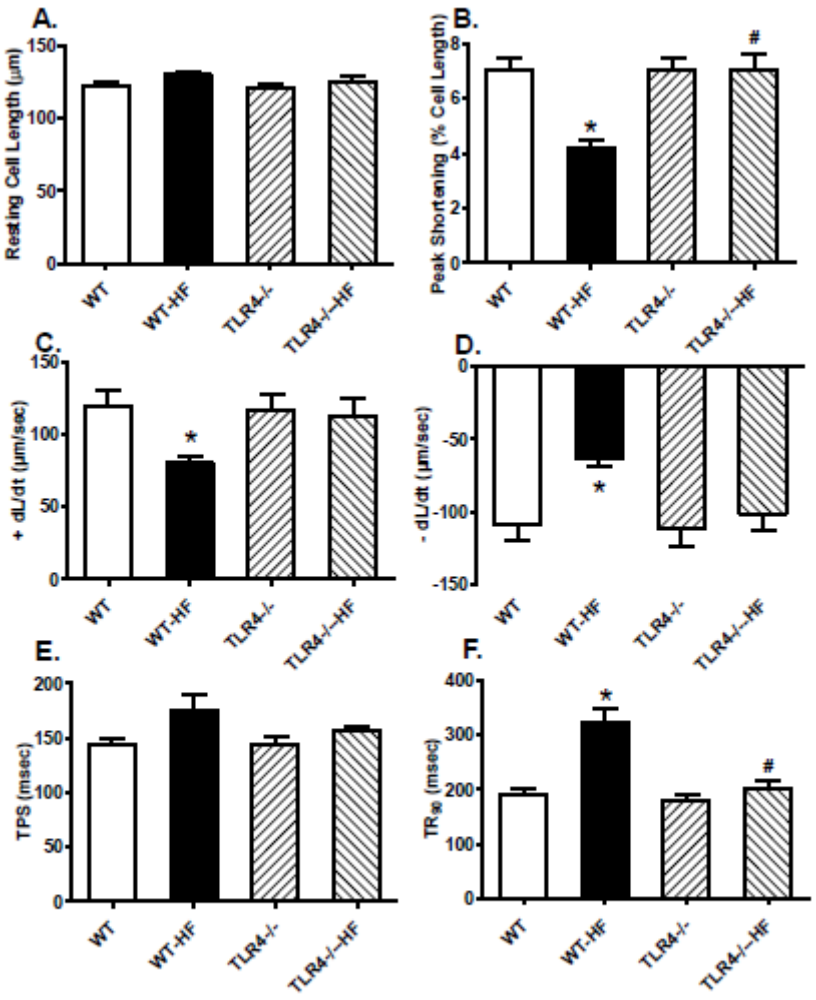
A.
Resting Cell Length (μm)
150
100
50
0
WT
WT-HF
TLR4-/-
TLR4-/--HF
B.
Peak Shortening (% Cell Length)
8
6
4
2
0
*
#
C.
+ dL/dt (μm/sec)
150
100
50
0
*
D.
- dL/dt (μm/sec)
0
-50
-100
-150
*
E.
TPS (msec)
200
150
100
50
0
F.
TR90 (msec)
400
300
200
100
0
*
#

Fig. 3

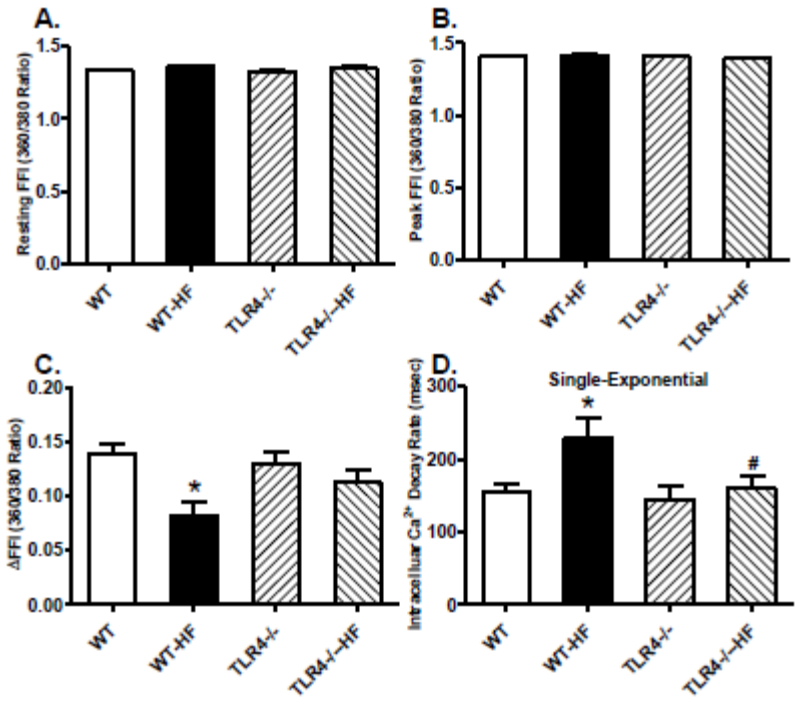
A.
Resting FFI (360/380 Ratio)
1.5
1.0
0.5
0.0
WT
WT-HF
TLR4-/-
TLR4-/-HF
B.
Peak FFI (360/380 Ratio)
1.5
1.0
0.5
0.0
WT
WT-HF
TLR4-/-
TLR4-/-HF
C.
ΔFFI (360/380 Ratio)
0.20
0.15
0.10
0.05
0.00
*
WT
WT-HF
TLR4-/-
TLR4-/-HF
D.
Single-Exponential
Intracellular Ca2+ Decay Rate (msec)
300
200
100
0
*
#
WT
WT-HF
TLR4-/-
TLR4-/-HF

Fig. 4

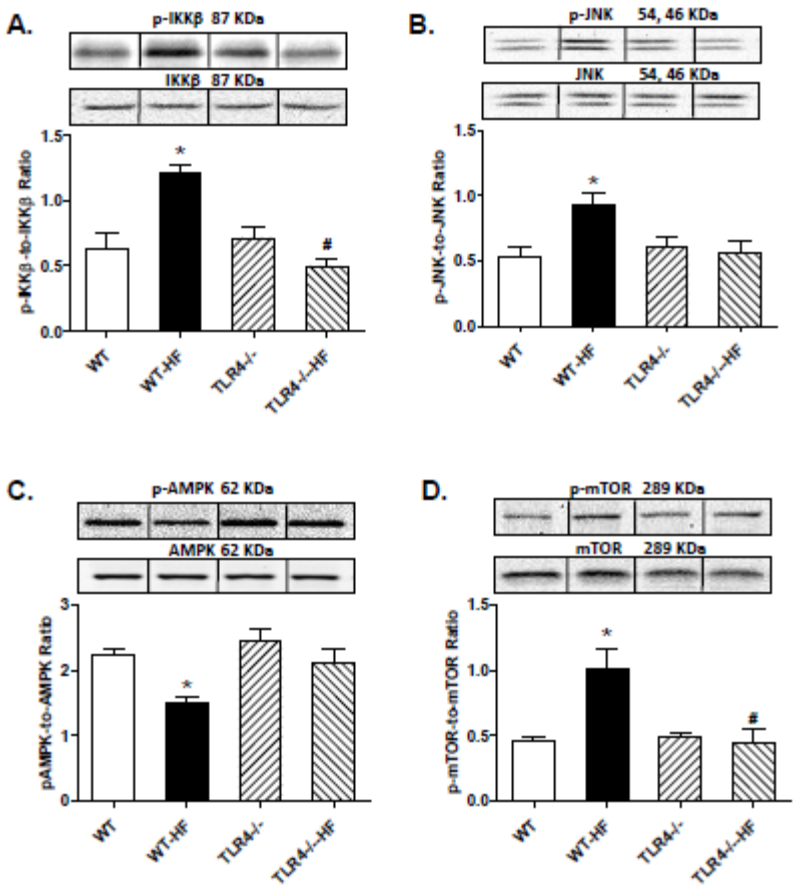
A.
p-IKKβ 87 KDa
IKKβ 87 KDa
p-IKKβ-to-IKKβ Ratio
1.5
1.0
0.5
0.0
*
#
WT
WT-HF
TLR4-/-
TLR4-/--HF
B.
p-JNK 54, 46 KDa
JNK 54, 46 KDa
p-JNK-to-JNK Ratio
1.5
1.0
0.5
0.0
*
WT
WT-HF
TLR4-/-
TLR4-/--HF
C.
p-AMPK 62 KDa
AMPK 62 KDa
pAMPK-to-AMPK Ratio
3
2
1
0
*
WT
WT-HF
TLR4-/-
TLR4-/--HF
D.
p-mTOR 289 KDa
mTOR 289 KDa
p-mTOR-to-mTOR Ratio
1.5
1.0
0.5
0.0
*
#
WT
WT-HF
TLR4-/-
TLR4-/--HF

Fig. 5

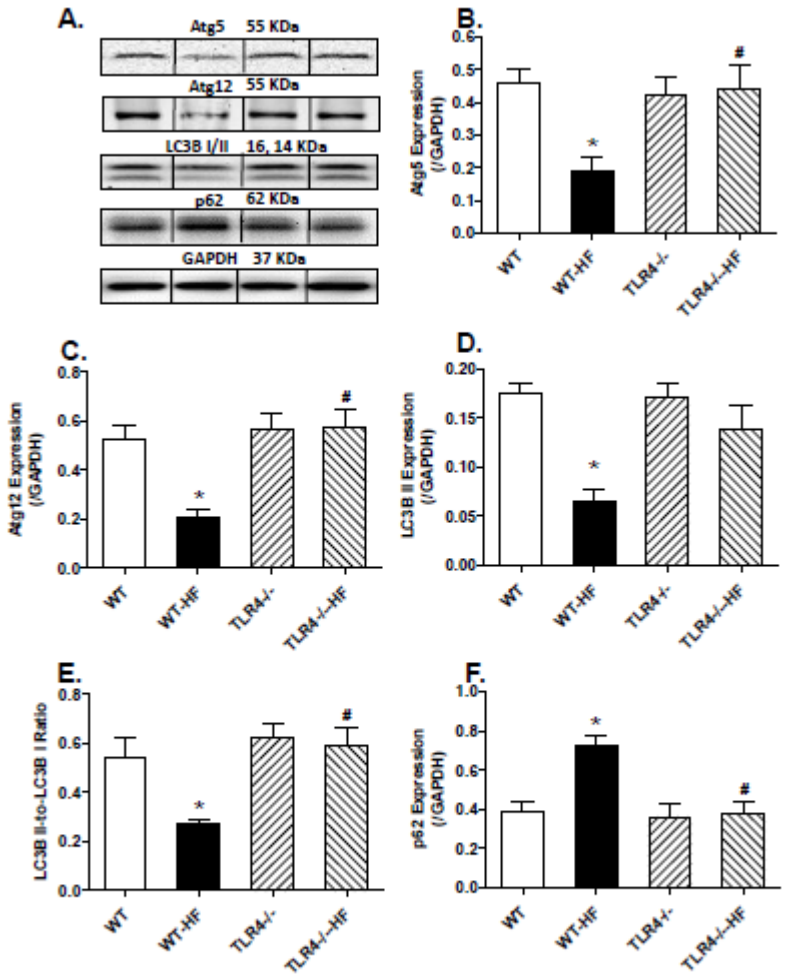
A.
Atg5 55 KDa
Atg12 55 KDa
LC3B I/II 16, 14 KDa
p62 62 KDa
GAPDH 37 KDa
B.
Atg5 Expression (/GAPDH)
C.
Atg12 Expression (/GAPDH)
D.
LC3B II Expression (/GAPDH)
E.
LC3B II-to-LC3B I Ratio
F.
p62 Expression (/GAPDH)
WT
WT-HF
TLR4-/-
TLR4-/-HF

Fig. 6

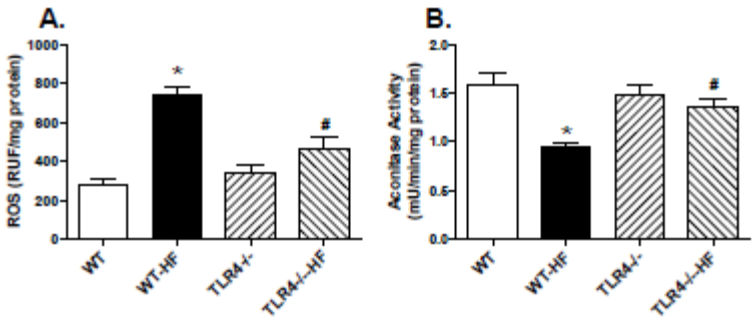
A.
ROS (RUF/mg protein)
1000
800
600
400
200
0
*
#
WT
WT-HF
TLR4-/-
TLR4-/-HF
B.
Aconitase Activity
(mU/min/mg protein)
2.0
1.5
1.0
0.5
0.0
*
#
WT
WT-HF
TLR4-/-
TLR4-/-HF

Fig. 7

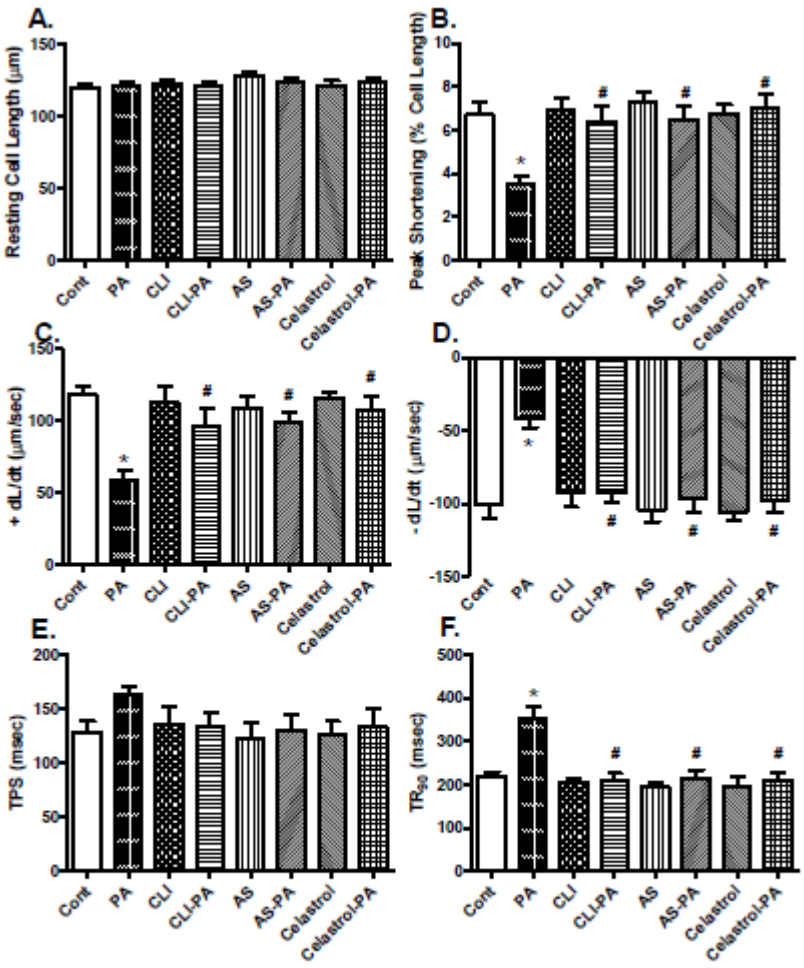
A.
Resting Cell Length (μm)
150
100
50
0
Cont
PA
CLI
CLI-PA
AS
AS-PA
Celastrol
Celastrol-PA
B.
Peak Shortening (% Cell Length)
10
8
6
4
2
0
*
#
C.
+ dL/dt (μm/sec)
*
#
D.
- dL/dt (μm/sec)
-50
-100
-150
E.
TPS (msec)
200
150
100
50
F.
TR90 (msec)
500
400
300

Fig. 8

Highlight

1.TLR4 knockout ameliorated high fat diet-induced cardiac contractile and intracellular Ca^{2+} anomalies

2. TLR4 knockout ameliorated high fat diet-induced cardiac injury through inhibition of inflammation and ROS, possibly through a NF-κB/JNK-dependent activation of autophagy.